Inorg. Chem. **2003**, *42*, 169–179

Syntheses, Crystal Structures, and Luminescent Properties of Lanthanide Complexes with Tripodal Ligands Bearing Benzimidazole and Pyridine Groups

Xiao-Ping Yang,[†,‡] Bei-Sheng Kang,*[,†] Wai-Kwok Wong,*[,‡] Cheng-Yong Su,[†] and Han-Qin Liu[†]

School of Chemistry and Chemical Engineering, Zhongshan University, Guangzhou 510275, People's Republic of China, and Chemistry Department, Hong Kong Baptist University, Kowloon Tong, Hong Kong

Received June 18, 2002

Two tripodal ligands, bis(2-benzimidazolylmethyl)(2-pyridylmethyl)amine (L^1) and bis(2-pyridylmethyl)(2-benzimidazolylmethyl)amine (L^2), were synthesized. With the third chromophoric ligand antipyrine (Antipy), three series of lanthanide(III) complexes were prepared: $[LnL^1(Antipy)_3](ClO_4)_3$ (series **A**), $[LnL^1(Antipy)Cl(H_2O)_2]Cl_2(H_2O)_2$ (series **B**), and $[LnL^2(NO_3)_3]$ (series **C**). The nitrate salt of the free ligand $H_2L^1 \cdot (NO_3)_2$ and six complexes were structurally characterized: **Pr^{3+}A**, **Y^{3+}A**, **Eu^{3+}B**, **Eu^{3+}C**, **Gd^{3+}C** and **Tb^{3+}C**, in which the two **A** and three **C** complexes are isomorphous. Crystallographic studies showed that tripodal ligands L^1 and L^2 exhibited a tripodal coordination mode and formed 1:1 complexes with all lanthanide metal ions. The coordination numbers of the lanthanide metal ions for the **A**, **B**, and **C** complexes were 7, 8, and 10, respectively. Conductivity studies on the **B** and **C** complexes in methanol showed that, in the former, the coordinated Cl^- dissociated to give 3:1 electrolytes and, in the latter, two coordinated NO_3^- ions dissociated to give 2:1 electrolytes. Detailed photophysical studies have been performed on the free ligands and their Gd(III), Eu(III), and Tb(III) complexes in several solvents. The results show a wide range in the emission properties of the complexes, which could be rationalized in terms of the coordination situation, the ^{3}LC level of the complexes, and the subtle variations in the steric properties of the ligands. In particular the **Eu^{3+}A** and **Tb^{3+}A** complexes, in which the central metal ions were wholly coordinated by chromophoric ligands of one L^1 and three antipyrine molecules, had relatively higher emission quantum yields than their corresponding **B** and **C** complexes.

Introduction

Over the past few years, considerable attention has been devoted to the design and synthesis of luminescent lanthanide complexes due to their potential use in biology and medicine, such as as catalysts for specific cleavage of RNA, stains for fluorescence imaging, and supramolecular devices.[1−6] In particular, Eu^{3+} and Tb^{3+} are attractive luminescent centers due to their visible long-lived emission. However, their photophysical properties markedly depend on their environment. To get an efficient cation emission, the chromophoric ligand should first absorb light strongly in the UV region and transfer it to the lanthanide ion efficiently, and second protect it from solvent molecules that can quench the central metal emission.[7−9] Many cryptand, calixarene, cyclodextrin, podand-type, and terpyridine-like ligands have been designed to isolate the ions from their surroundings.[7,10−12]

* Authors to whom correspondence should be addressed. E-mail: lhq@zsu.edu.cn (B.-S.K.); wkwong@hkbu.edu.hk (W.-K.W.).
† Zhongshan University.
‡ Hong Kong Baptist University.

(1) Tangay, J.; Suib, S. L. *Catal. Rev. Sci. Eng.* **1987**, *29*, 1.
(2) Parker, D.; Williams, J. A. G. *J. Chem. Soc., Dalton Trans.* **1996**, 3613.
(3) Mathis, G. *Clin. Chem.* **1995**, *41*, 1391.
(4) Komiyama, M. J. *J. Biochem.* **1995**, *118*, 665.
(5) McGehee, M. D.; Bergstedt, T.; Zhang, C.; Saab, A. P.; O'Regan, M. B.; Bazan, G. C.; Strdanov, V. I.; Heeger, A. *J. Adv. Mater.* **1999**, *11*, 1349.
(6) Yang, W. Y.; Chen, L.; Wang, S. *Inorg. Chem.* **2001**, *40*, 507.
(7) Sabbatini, N.; Guardigli, M.; Lehn, J. M. *Coord. Chem. Rev.* **1993**, *123*, 201.
(8) Alison, S. G.-P.; Ishenkumba, A. K.; Andrew, J. P. W.; David, J. W. *Inorg. Chem.* **1999**, *38*, 1745.
(9) Peter, L. J.; Angelo, J. A.; John, C. J.; Jon, A. M.; Elefteria, P.; Leigh, H. R.; Michael, D. W. *Inorg. Chem.* **1997**, *36*, 10.
(10) Ohash, K.; Yoshikawa, S.; Akutsu, B.; Nakano, Y.; Usui, Y. *Anal. Sci.* **1990**, 827.
(11) Sabbatini et al. *Advances in Photochemistry*; Neckers, Volman, von Bunau, Eds.; Wiley: New York, 1997; Vol. 23, p 213.

10.1021/ic025799p CCC: $25.00
Published on Web 11/23/2002

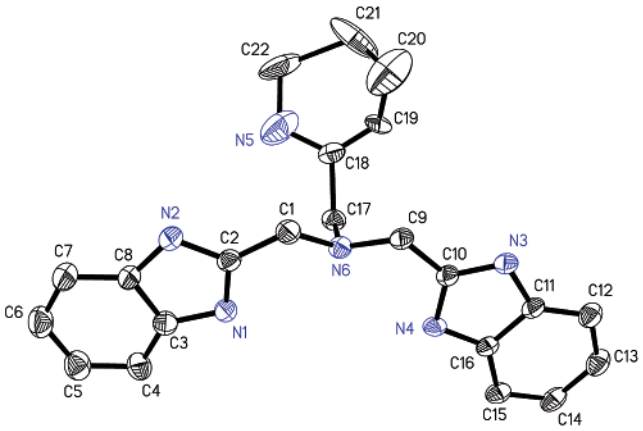

Figure 1. Crystal structure of the free ligand $H_2L^1 \cdot (NO_3)_2$.

As contrast agents for magnetic resonance imaging (MRI), the tripodal ligands derived from the Schiff base condensation with tris(2-aminoethyl)amine have attracted much attention recently.[13−16] With three suitably designed arms, the tripodal ligands could shield the encapsulated lanthanide ions from interaction with the surroundings, and by deliberate incorporation of appropriate multiple absorption groups suitable for energy transfer, they could be used to develop strong luminescent lanthanide complexes. We have been interested in the synthesis and characterization of lanthanide complexes with tripodal ligands incorporating a benzimidazole group,[17−21] which allows easy derivation and potentially strong $\pi-\pi$ stacking interaction to form supramolecular structures. In particular, we have recently synthesized a tripodal ligand, bis(2-benzimidazolylmethyl)(2-pyridylmethyl)amine (L^1; Figure 1), and its two series of lanthanide complexes ($[LnL^1(NO_3)_3] \cdot C_2H_5OH$ and $[LnL^1Cl_3(H_2O)] \cdot C_2H_5OH$), in which the metal ions are coordinated with one L^1 and three anions (NO_3^- or Cl^-).[22] In an effort to completely encapsulate the lanthanide ion with chromophoric ligands and increase its luminescence, herein, besides the tripodal ligand L^1, we introduce a second organic ligand, antipyrine, instead of those anions (Chart 1), and synthesize two series of their lanthanide complexes. To examine the ligand-to-metal energy-transfer process of these kinds of lanthanide complexes in more detail, in this paper, we also present the syntheses and photophysical studies of some nitrate-coordinated lanthanide complexes with another similar tripodal ligand, bis(2-pyridylmethyl)(2-benzimidazolylmethyl)amine (L^2; Chart 1).

Chart 1. (a) Tripodal Ligand L^1, (b) Tripodal Ligand L^2, and (*c*) Antipyrine

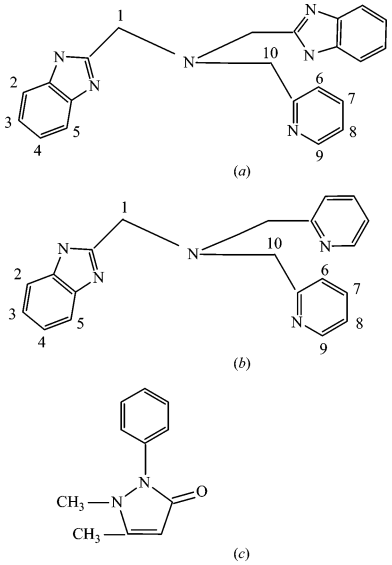

Experimental Section

Materials. Solvents and starting materials were purchased commercially and used without further purification unless otherwise noted. Hydrated lanthanide nitrates, chlorides, and perchlorates were prepared from the corresponding oxides according to literature methods.[23]

Caution! Lanthanide perchlorates combined with organic ligands are potentially explosive and should be handled in small quantities and with adequate precautions.

Methods and Instrumentation. Elemental analyses (C, H, N) were carried out on a Varian EL elemental analyzer. ^{1}H NMR spectra were recorded on a Varian-500 NMR spectrometer with $SiMe_4$ as an internal standard, UV spectra on a SHIMADZU UV-2501PC spectrophotometer, infrared spectra from 4000 to 400 cm^{-1} on a Bruker EQINOX 55 FT-IR spectrometer, and fast atom bombardment (FAB) mass spectra on a VG ZAB-HS mass spectrometer with 3-nitrobenzyl alcohol as matrix. Conductivity measurements were carried out with a DDS-11 conductivity bridge for 10^{-3} mol dm^{-1} solutions in CH_3CN and CH_3OH.

Preparation of Bis(2-benzimidazolylmethyl)(2-pyridylmethyl)amine (L^1) and $[LnL^1(NO_3)_3] \cdot C_2H_5OH$ (LnL^1; Ln = Tb, Gd, Eu). The ligand L^1 and its nitrate-coordinated lanthanide complexes LnL^1 were synthesized according to procedures previously described.[22] We obtained a pale yellow single crystal of $(H_2L^1) \cdot (NO_3)_2$ while attempting to get the crystal $[LnL^1(Antipy)_3](NO_3)_3$ in air at room temperature from an ethanol solution of $Tb(NO_3)_3$, L^1, and antipyrine in a 1:1:3 molar ratio.

Preparation of $[LnL^1(Antipy)_3](ClO_4)_3$ (Series A; Ln = La, Pr, Eu, Gd, Tb, Y). To a methanol solution (10 mL) of L^1 (0.018 g, 0.05 mmol) and $Ln(ClO_4)_3 \cdot 11H_2O$ (0.05 mmol) was added a methanol solution (5 mL) of antipyrine (0.029 g, 0.15 mmol) slowly. The resulting solution was stirred and heated for 30 min. After filtration, the solution was left standing overnight at room temper-

(12) Alpha, B.; Lehn, J.-M.; Mathis, G. *Angew. Chem., Int. Ed. Engl.* **1987**, *26*, 266.
(13) Bretonnière, Y.; Mazzanti, M.; Pécaut, J.; Dunand, F. A.; Merbach, A. E. *Inorg. Chem.* **2001**, *40*, 6737.
(14) Liu, S.; Getmini, L.; Remg, A. J.; Thompson, R. C.; Orvig, C. *J. Am. Chem. Soc.* **1992**, *114*, 6081.
(15) Archibald, S. J.; Blake, A. J.; Parsons, S.; Scrrödon M.; Winpenny, R. E. P. *J. Chem. Soc., Dalton Trans.* **1997**, 173.
(16) Archibald, S. J.; Blake, A. J.; Scrrödon M.; Winpenny, R. E. P. *Chem. Commun.* **1994**, 1669.
(17) Su, C.-Y.; Yang, X.-P.; Kang, B.-S.; Mak, T. C. W. *Angew. Chem., Int. Ed.* **2001**, *40*, 1725.
(18) Su, C.-Y.; Kang, B.-S.; Liu, H.-Q.; Wang, Q.-G.; Chen, Z.-N.; Lu, Z.-N.; Tong, Y.-X.; Mak, T. C. W. *Inorg. Chem.* **1999**, *38*, 1374.
(19) Su, C.-Y.; Kang, B.-S.; Liu, H.-Q.; Wang, Q.-G.; Mak, T. C. W. *Chem. Commun.* **1998**, 1551.
(20) Wietzke, R.; Mazzanti, M.; Latour J.-M.; Pécaut, J. *Chem. Commun.* **1999**, 209.
(21) Wietzke, R.; Mazzanti, M.; Latour J.-M.; Pécaut, J.; Cordier, P.-Y.; Madic, C. *Inorg. Chem.* **1998**, *37*, 6690.
(22) Yang, X.-P.; Su, C.-Y.; Kang, B.-S.; Fong, X.-L.; Xiao, W.-L.; Liu, H.-Q. *J. Chem. Soc., Dalton Trans.* **2000**, 3253.
(23) Desreux, J. F. In *Lanthanide Probes in Life, Chemical and Earth Sciences*; Choppin, G. R., Bünzli, J.-C. G., Eds.; Elsevier Publishing Co.: Amsterdam, 1989; Chapter 2, p 43.

Table 1. Mass, Elemental Analytical, IR Spectral, and Conductivity Data for the Complexes

		elemental analyses[a] (%)			IR (ν_{max}/cm^{-1})			Λ_M[e]/Ω^{-1} cm^2 mol^{-1}	
	FAB MS, *m*/*z*	C	H	N	$\nu_{C=N}$[b]	$\nu_{C=O}$[c]	ν_{NO}[d]	CH_3OH	CH_3CN
L^2	330 $[M + H]^+$	72.67 (72.93)	6.02 (5.81)	21.13 (21.26)	(1620, 1589)				
La^{3+}A	1271 $\{LaL^1(Antipy)_3(ClO_4)_2\}$	47.91 (48.21)	4.47 (4.12)	12.11 (12.27)	(1620, 1604)	1628			
Pr^{3+}A	1274 $\{PrL^1(Antipy)_3(ClO_4)_2\}$	48.01 (48.14)	4.52 (4.11)	11.89 (12.25)	(1619, 1603)	1629			
Eu^{3+}A	1284 $\{EuL^1(Antipy)_3(ClO_4)_2\}$	47.51 (47.75)	4.46 (4.08)	11.97 (12.15)	(1620, 1603)	1632			
Gd^{3+}A		47.11 (47.57)	4.51 (4.06)	11.85 (12.10)	(1621, 1604)	1631			
Tb^{3+}A	1291 $\{TbL^1(Antipy)_3(ClO_4)_2\}$	47.32 (47.51)	4.33 (4.06)	11.91 (12.09)	(1621, 1602)	1630			
Y^{3+}A		49.35 (50.03)	4.52 (4.27)	12.34 (12.73)	(1622, 1602)	1631			
Eu^{3+}B	780 $\{EuL^1(Antipy)Cl_2\}$	44.55 (44.69)	4.16 (4.55)	12.57 (12.64)	(1618, 1599)	1625		309.1	203.2
Gd^{3+}B	785 $\{GdL^1(Antipy)Cl_2\}$	44.01 (44.44)	4.21 (4.52)	12.78 (12.57)	(1619, 1600)	1629		352.6	185.1
Tb^{3+}B	787 $\{TbL^1(Antipy)Cl_2\}$	43.92 (44.38)	4.19 (4.52)	12.72 (12.56)	(1620, 1602)	1628		330.7	179.6
La^{3+}C	593 $\{LaL^2(NO_3)_2\}$	36.68 (36.71)	3.22 (2.93)	17.57 (17.13)	(1623, 1605)		(1294, 1462)	203.8	<2
Eu^{3+}C	606 $\{EuL^2(NO_3)_2\}$	35.92 (35.99)	3.19 (2.87)	16.90 (16.79)	(1622, 1602)		(1301, 1460)	187.2	<2
Gd^{3+}C	611 $\{GdL^2(NO_3)_2\}$	35.31 (35.71)	3.07 (2.85)	16.83 (16.66)	(1621, 1604)		(1295, 1473)	218.9	<2
Tb^{3+}C	613 $\{TbL^2(NO_3)_2\}$	35.41 (35.62)	2.95 (2.84)	16.44 (16.62)	(1621, 1606)		(1300, 1475)	223.5	<2

[a] Data in parentheses are calculated values. [b] Imidazole ring. [c] Antipyrine. [d] Nitrate. [e] Measured at 298 K.

Table 2. Crystal Data and Structure Refinement for the Free L^2 and Six Complexes

	$H_2L^1\cdot(NO_3)_2$	**Pr^{3+}A**	**Y^{3+}A**	**Eu^{3+}B**	**Eu^{3+}C**	**Gd^{3+}C**	**Tb^{3+}C**
empirical formula	$C_{22}H_{22}N_8O_6$	$C_{55}H_{56}N_{12}O_{15}Cl_3Pr$	$C_{55}H_{56}N_{12}O_{15}Cl_3Y$	$C_{33}H_{40}N_8O_5Cl_3Eu$	$C_{20}H_{19}N_8O_9Eu$	$C_{20}H_{19}N_8O_9Gd$	$C_{20}H_{19}N_8O_9Tb$
fw	494.60	1372.37	1320.38	887.04	667.38	672.68	674.34
cryst syst	monoclinic	monoclinic	monoclinic	triclinic	monoclinic	monoclinic	rhombohedral
space group	$P2_1/c$	$P2_1/m$	$P2_1/m$	$P\bar{1}$	$P2_1/n$	$P2_1/n$	$R\bar{3}$
a, Å	8.176(2)	12.530(2)	12.487(2)	10.400(2)	11.689(2)	11.6761(19)	17.275(5)
b, Å	18.447(3)	41.536(6)	41.337(6)	10.853(2)	13.667(3)	13.659(2)	17.275(5)
c, Å	15.437(3)	13.816(2)	13.729(2)	17.598(3)	16.122(3)	16.115(3)	17.275(5)
α, deg	90	90	90	78.639(3)	90	90	99.268(4)
β, deg	92.641(4)	115.35	115.36	81.833(3)	106.04	106.049(4)	99.268(4)
γ, deg	90	90	90	84.934(3)	90	90	99.268(4)
V, Å^3	2325.8(7)	6498(2)	6404(2)	1924.0(5)	2475.3(8)	2469.9(7)	4928(2)
Z	4	4	4	2	4	4	6
D_{calcd}, g cm^{-3}	1.401	1.403	1.370	1.531	1.791	1.809	1.412
temp, K	294	293	293	293	293	293	293
μ, mm^{-1}	0.106	0.943	1.107	1.888	2.600	2.752	2.205
θ range, deg	2.49−27.63	9.74−27.09	9.75−25.06	1.92−27.58	1.92−27.07	1.92−27.55	3.94−30.00
no. of reflns measured	5348	13609	10653	10449	5393	5692	9418
no. of reflns used	1317	5509	3027	8095	3095	2185	3597
no. of params	371	859	817	897	343	344	362
final R^a ($I > 2\sigma(I)$)	R1 = 0.0502	R1 = 0.0965	R1 = 0.0789	R1 = 0.0418	R1 = 0.0459	R1 = 0.0520	R1 = 0.0726
	wR2 = 0.1123	wR2 = 0.2136	wR2 = 0.1761	wR2 = 0.0965	wR2 = 0.0982	wR2 = 0.1029	wR2 = 0.1809
R^a (all data)	R1 = 0.2459	R1 = 0.2162	R1 = 0.3119	R1 = 0.0613	R1 = 0.0977	R1 = 0.1419	R1 = 0.2080
	wR2 = 0.1765	wR2 = 0.2613	wR2 = 0.2639	wR2 = 0.1043	wR2 = 0.1250	wR2 = 0.1209	wR2 = 0.2713
goodness of fit on F^2	0.791	0.973	0.877	0.953	1.008	0.760	1.027

[a] $R1 = \sum||F_o| - |F_c||/\sum|F_o|$. $wR2 = [\sum w[(F_o^2 - F_c^2)^2]/\sum|[w(F_o^2)^2]]^{1/2}$. $w = 1/[\sigma^2(F_o^2) + (0.075P)^2]$, where $P = [\max(F_o^2,0) + 2F_c^2]/3$.

ature to afford a pale yellow solid, which was filtered, washed three times with methanol and diethyl ether successively, and dried over $CaCl_2$ in a desiccator for 1 day to give the product in 50−70% yield. Pale yellow single crystals were obtained by vapor diffusion of diethyl ether into the ethanol solution.

Preparation of $[LnL^1(Antipy)Cl(H_2O)_2]Cl_2(H_2O)_2$ (Series B; Ln = Eu, Gd, Tb). In a similar method, a solution of antipyrine (0.029 g, 0.15 mmol) in 5 mL of methanol was added to a methanol solution (10 mL) of L^1 (0.018 g, 0.05 mmol) and $LnCl_3\cdot6H_2O$ (0.05 mmol). The resulting solution was treated as above, and the yield was in the range of 40−60%. Pale yellow single crystals were obtained as in series **A**.

Preparation of Bis(2-pyridylmethyl)(2-benzimidazolylmethyl)amine (L^2). The preparation was similar to the recently reported procedure.[24] Yield: 53%. IR (KBr, cm^{-1}): 3411 (br), 3050 (br), 1589 (s), 1510 (m), 1433 (s), 1330 (m), 1273 (m), 995 (w), 744 (s). FAB MS and elemental analysis data are summarized in Table 1 and ^{1}H NMR data in Table 4

Preparation of $[LnL^2(NO_3)_3]$ (Series C; Ln = La, Eu, Gd, Tb). To a clear solution of L^2 (0.016 g, 0.05 mmol) in ethanol (5 mL) was added slowly a solution of $Ln(NO_3)_3\cdot5H_2O$ (0.05 mmol) in 5 mL of ethanol. The resulting solution was treated as in series **A**, and the yield was in the range 50−70%. Pale yellow single crystals were obtained as in series **A**.

X-ray Crystallography. Details of crystallographic parameters, data collection, and refinements are listed in Table 2. Intensities were collected on a Bruker SMART 1000 CCD diffractometer with graphite-monochromated Mo Kα radiation ($\lambda = 0.71073$ Å) at 293 K. Absorption corrections were applied using ABSCOR.[25] The structures were solved by direct methods and refined anisotropically by the full-matrix least-squares technique using the SHELX 97 program package.[26] The coordinates of the non-hydrogen atoms were refined anisotropically, while hydrogen atoms were included in the calculation isotropically but not refined. Neutral atom

(24) Matthias, P.; Mark, D.; Florian, S.; Kristin, Z.; Felizitas, K. M.; Bernt, K. *J. Chem. Soc., Dalton Trans.* **2001**, 828.

(25) Higashi, T. *ABSCOR, An Empirical Absorption Correction Based on Fourier Coefficient Fitting*; Rigaku Corp.: Tokyo, 1995.

(26) Sheldrick, G. M. *SHELX 97, A software package for the solution and refinement of X-ray data*; University of Göttingen: Göttingen, Germany, 1997.

scattering factors were taken from Cromer and Waber.[27] Full details are available in the Supporting Information.

Photophysical Studies. The solvents used for the photophysical investigations were the following: (i) distilled acetonitrile and methanol from CaH_2 and $Mg(OMe)_2$, respectively; (ii) distilled water from a Millipore Milli-RO 15 purification system; (iii) 99.5% isotopically pure CD_3OD and D_2O (Carlo Erba). Absorption spectra were obtained on a SHIMADZU UV-2501PC spectrophotometer and emission and excitation spectra on a HITACHI 850 spectrometer. Fluorescence quantum yields were determined following the method described by Nakamaru et al., using $[Ru(bipy)_3]Cl_2$ (bipy = 2,2′-bipyridine; $\Phi = 0.028$ in water; $\lambda_{exc} = 436$ nm)[28] as standard for the Eu^{3+} complex, and quinine sulfate ($\Phi = 0.546$ in 0.5 mol dm^{-3} H_2SO_4; $\lambda_{exc} = 365$ nm)[29] for the Tb^{3+} complex. The luminescence decays were recorded using a pumped dye laser (Lambda Physics model FL2002) as the excitation source. The number of coordinated solvent molecules (q) for the Eu^{3+} and Tb^{3+} complexes was calculated from the Horrocks equation $q = n(\tau_H^{-1} - \tau_D^{-1})$, where τ_H is the lifetime in the protonated solvent (water or CH_3OH) and τ_D that in the corresponding deuterated solvent and the value of n is 1.05 (Eu^{3+} in H_2O/D_2O), 4.2 (Tb^{3+} in H_2O/D_2O), 2.1 (Eu^{3+} in CH_3OH/CD_3OD), or 8.4 (Tb^{3+} in CH_3OH/CD_3OD).[7]

Results and Discussion

Synthesis. The syntheses of free ligand L^1 and its nitrate-coordinated complexes $[Ln(NO_3)_3L^1]$ (Ln = Eu, Gd, Tb) have been reported before.[22] The ligand L^2 was synthesized using procedures similar to those for L^1 by first condensing aminoacetic acid with *o*-phenylenediamine and then reacting it with 2-picolyl chloride hydrochloride. The effect of anions on the formation of the complexes was examined by treating lanthanide salts ($LnX_3 \cdot xH_2O$) (X = Cl, ClO_4, and NO_3) with L^1 or L^2 and antipyrine in a 1:1:3 molar ratio. Elemental analyses and FAB MS data confirmed that L^1 and L^2 formed 1:1 complexes with lanthanide ions (Table 1). On the basis of the crystal structures of lanthanide complexes and the similarity of their IR spectra, three series of complexes of general formulas $[LnL^1(Antipy)_3](ClO_4)_3$ (series **A**), $[LnL^1(Antipy)Cl(H_2O)_2]Cl_2(H_2O)_2$ (series **B**), and $[LnL^2(NO_3)_3]$ (series **C**) were obtained.

Crystal Structures. The crystallographic data for $(H_2L^1)\cdot(NO_3)_2$ and complexes $\mathbf{Pr^{3+}A}$, $\mathbf{Y^{3+}A}$, $\mathbf{Eu^{3+}B}$, $\mathbf{Eu^{3+}C}$, $\mathbf{Gd^{3+}C}$, and $\mathbf{Tb^{3+}C}$ are listed in Table 2. The structures and atomic numbering schemes of $(H_2L^1)\cdot(NO_3)_2$, $\mathbf{Pr^{3+}A}$, $\mathbf{Eu^{3+}B}$, and $\mathbf{Tb^{3+}C}$ are shown in Figures 1, 3, 4, and 6, respectively, while the others are not displayed as they are isomorphous with the above. Despite the fact that some lanthanide complexes of L^1 have been studied, no crystal structure of the free ligand has been reported to date. As shown in Figure 1, with two benzimidazolyl groups almost coplanar (dihedral angle 3.5°), the free L^1 exhibits a "T-like" configuration which results in intermolecular $\pi-\pi$ stacking interaction between two neighboring molecules closing face-to-face (average center-to-center distance between two adjacent benzimidazolyl groups 3.705 Å, dihedral angle 7.1°) (Figure 2). As discussed in previous studies,[22] compared with the "fanlike" configuration shown in LnL^1, the "T-like" configuration has a larger steric effect, which is offset by this kind of intermolecular interaction. The pyridyl ring of L^1 does not form $\pi-\pi$ stacking with the benzimidazolyl ring, in agreement with the fact that the benzimidazolyl ring has a higher conjugated system than the pyridyl ring and is consequently easier to form.

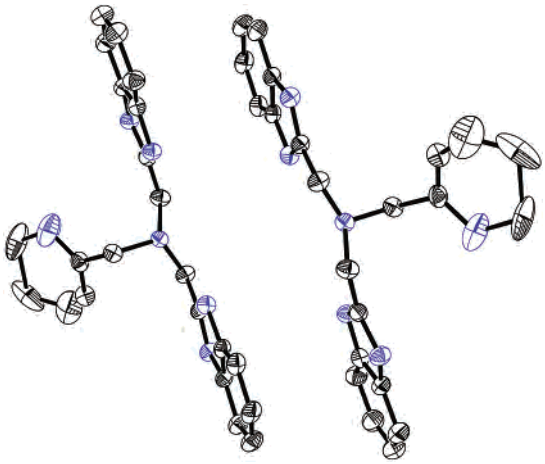

Figure 2. Intermolecular $\pi-\pi$ interaction in the free ligand $H_2L^1\cdot(NO_3)_2$.

Complexes $\mathbf{Pr^{3+}A}$ and $\mathbf{Y^{3+}A}$ are isomorphous, with only very minor differences in their comparative geometries reflecting the normal lanthanide(III) contraction effects. The central metal ions are 7-coordinated, surrounded by four nitrogen atoms of the tetradentate ligand L^1 and three oxygen atoms of the three antipyrine molecules. Since the coordination environment of the metal ion is blocked by three bulky antipyrine molecules, no water molecule enters into the coordination cavity and the central metal ion is wholly coordinated by organic ligands. However, in the crystal structure of $\mathbf{Eu^{3+}B}$, besides the four nitrogen atoms of the ligand L^1 and one oxygen atom of the antipyine molecule, there is one Cl^-, which is smaller than ClO_4^- and easily enters the coordination sphere, and two water molecules coordinated, resulting in an 8-coordinated metal ion. Since coordinated solvent molecules, especially water or alcohol, can efficiently quench lanthanide luminescence, the **A** and **B** complexes show quite different luminescence properties (see later). Comparison of these structures shows that the anions (Cl^- and ClO_4^-) have a substantial effect on the structure, and the ability for antipyrine molecules to exclude solvent molecules from the first coordination sphere in the **A** complexes is an important criterion in the design of a luminescent lanthanide complex.[7]

Complexes $\mathbf{Eu^{3+}C}$, $\mathbf{Gd^{3+}C}$, and $\mathbf{Tb^{3+}C}$ are also isomorphous and composed of a neutral $[LnL^2(NO_3)_3]$ (Ln = Eu, Gd or Tb) entity with the central metal ion 10-coordinated, being linked to four nitrogen atoms of the tetradentate ligand L^2 and six oxygen atoms of the three bidentate NO_3^- groups. Due to the small bite angle in a NO_3^- group, the donor atoms of bidentate nitrate are closer together than those of two independent monodentate ligands such as antipyrine and Cl^-, so the nitrate-based lanthanide **C** complexes have a high coordination number. The low coordination number of the

(27) Cromer D. T.; Waber, J. T. *International Tables for X-ray Crystallography*; Kynoch Press: Birmingham, 1974; Vol. 4, Table 2.2A.
(28) Nakamaru, K. *Bull. Soc. Chem. Jpn.* **1982**, *5*, 2697.
(29) Meech S. R.; Philips, D. J. *J. Photochem.* **1983**, *23*, 193.

Table 3. Selected Band Lengths (Å) for All Crystal Structures and Angles (deg) for $H_2L^1\cdot(NO_3)_2$, $\mathbf{Pr^{3+}A}$, $\mathbf{Eu^{3+}B}$, and $\mathbf{Eu^{3+}C}$

				$H_2L^1\cdot(NO_3)_2$					
O(1)−N(7)	1.223(4)	N(2)−C(2)	1.328(4)	N(6)−C(9)	1.442(4)	C(6)−C(7)	1.372(6)	C(15)−C(16)	1.393(5)
O(2)−N(7)	1.251(4)	N(2)−C(8)	1.369(4)	N(6)−C(1)	1.450(4)	C(7)−C(8)	1.377(5)	C(17)−C(18)	1.522(5)
O(3)−N(7)	1.202(4)	N(3)−C(10)	1.297(4)	N(6)−C(17)	1.475(4)	C(9)−C(10)	1.489(5)	C(18)−C(19)	1.367(17)
O(4)−N(8)	1.275(4)	N(3)−C(11)	1.394(4)	C(1)−C(2)	1.477(5)	C(11)−C(12)	1.370(5)	C(19)−C(20)	1.44(3)
O(5)−N(8)	1.223(4)	N(4)−C(10)	1.344(4)	C(3)−C(4)	1.370(5)	C(11)−C(16)	1.384(5)	C(20)−C(21)	1.28(4)
O(6)−N(8)	1.219(4)	N(4)−C(16)	1.390(4)	C(3)−C(8)	1.400(6)	C(12)−C(13)	1.382(5)	C(21)−C(22)	1.30(3)
N(1)−C(2)	1.324(4)	N(5)−C(22)	1.41(3)	C(4)−C(5)	1.378(5)	C(13)−C(14)	1.373(5)		
N(1)−C(3)	1.381(4)	N(5)−C(18)	1.453(18)	C(5)−C(6)	1.383(6)	C(14)−C(15)	1.369(5)		
C(2)−N(1)−C(3)	109.4(4)	O(1)−N(7)−O(2)	119.7(4)	N(1)−C(3)−C(8)	105.6(4)	N(3)−C(10)−C(9)	124.9(4)	C(11)−C(16)−C(15)	121.4(4)
C(2)−N(2)−C(8)	109.3(3)	O(6)−N(8)−O(5)	123.5(4)	C(3)−C(4)−C(5)	117.1(5)	N(4)−C(10)−C(9)	125.2(3)	N(4)−C(16)−C(15)	131.6(4)
C(10)−N(3)−C(11)	110.1(3)	O(6)−N(8)−O(4)	118.1(4)	C(4)−C(5)−C(6)	121.6(5)	C(12)−C(11)−C(16)	121.9(4)	N(6)−C(17)−C(18)	117.4(3)
C(10)−N(4)−C(16)	107.8(3)	O(5)−N(8)−O(4)	118.3(4)	C(7)−C(6)−C(5)	121.4(5)	C(12)−C(11)−N(3)	132.7(4)	C(19)−C(18)−N(5)	125.9(11)
C(22)−N(5)−C(18)	114.9(17)	N(6)−C(1)−C(2)	112.1(3)	C(6)−C(7)−C(8)	117.6(5)	C(16)−C(11)−N(3)	105.4(4)	C(19)−C(18)−C(17)	117.3(10)
C(9)−N(6)−C(1)	113.4(3)	N(1)−C(2)−N(2)	109.1(4)	N(2)−C(8)−C(7)	132.7(5)	C(11)−C(12)−C(13)	116.1(4)	N(5)−C(18)−C(17)	115.0(9)
C(9)−N(6)−C(17)	113.7(3)	N(1)−C(2)−C(1)	125.9(4)	N(2)−C(8)−C(3)	106.6(4)	C(14)−C(13)−C(12)	122.5(4)	C(18)−C(19)−C(20)	105.8(18)
C(1)−N(6)−C(17)	113.4(3)	N(2)−C(2)−C(1)	124.9(4)	C(7)−C(8)−C(3)	120.7(5)	C(15)−C(14)−C(13)	121.7(4)	C(21)−C(20)−C(19)	130(2)
O(3)−N(7)−O(1)	119.4(4)	C(4)−C(3)−N(1)	132.8(4)	N(6)−C(9)−C(10)	111.3(3)	C(14)−C(15)−C(16)	116.4(4)	C(20)−C(21)−C(22)	117.9(18)
O(3)−N(7)−O(2)	120.9(4)	C(4)−C(3)−C(8)	121.6(4)	N(3)−C(10)−N(4)	109.8(3)	C(11)−C(16)−N(4)	107.0(3)	C(21)−C(22)−N(5)	118(2)
				$Pr^{3+}A$					
Pr(1)−O(3)	2.252(6)	Pr(1)−O(1)	2.336(8)	Pr(1)−N(3)	2.542(8)	Pr(1)−N(6)	2.770(8)		
Pr(1)−O(2)	2.313(6)	Pr(1)−N(1)	2.520(8)	Pr(1)−N(5)	2.630(9)				
O(3)−Pr(1)−O(2)	93.1(2)	O(1)Pr(1)−N(1)	82.4(3)	O(3)−Pr(1)−N(5)	82.0(3)	O(3)−Pr(1)−N(6)	122.7(2)	N(5)−Pr(1)−N(6)	61.7(3)
O(3)−Pr(1)−O(1)	90.0(2)	O(3)−Pr(1)-N(3)	84.4(2)	O(2)−Pr(1)−N(5)	82.3(3)	O(2)−Pr(1)−N(6)	121.1(2)		
O(2)−Pr(1)−O(1)	88.8(3)	O(2)−Pr(1)−N(3)	176.1(2)	O(1)−Pr(1)−N(5)	167.6(3)	O(1)−Pr(1)−N(6)	130.6(3)		
O(3)−Pr(1)−N(1)	172.3(3)	O(1)−Pr(1)−N(3)	88.3(3)	N(1)−Pr(1)−N(5)	105.2(3)	N(1)−Pr(1)−N(6)	64.2(3)		
O(2)−Pr(1)−N(1)	85.3(2)	N(1)−Pr(1)−N(3)	96.8(3)	N(3)−Pr(1)−N(5)	100.3(3)	N(3)−Pr(1)−N(6)	62.7(2)		
				$Y^{3+}A$					
Y(1)−O(3)	2.183(9)	Y(1)−O(1)	2.200(8)	Y(1)−N(3)	2.449(8)	Y(1)−N(6)	2.678(8)		
Y(1)−O(2)	2.199(7)	Y(1)−N(1)	2.440(9)	Y(1)−N(5)	2.561(11)				
				$Eu^{3+}B$					
Eu(1)−O(1)	2.265(4)	Eu(1)−O(1W)	2.389(3)	Eu(1)−N(3)	2.436(5)	Eu(1)−N(6)	2.728(3)		
Eu(1)−O(2W)	2.366(4)	Eu(1)−N(1)	2.423(5)	Eu(1)−N(5)	2.548(5)	Eu(1)−Cl(1)	2.7220(16)		
O(1)−Eu(1)−O(2W)	78.93(14)	O(1)−Eu(1)−N(3)	153.65(14)	O(1W)−Eu(1)−N(5)	146.98(15)	N(1)−Eu(1)−Cl(1)	139.02(11)	N(1)−Eu(1)−N(6)	65.93(13)
O(1)−Eu(1)−O(1W)	78.40(12)	O(2W)−Eu(1)−N(3)	88.16(16)	N(1)−Eu(1)−N(5)	67.69(16)	N(3)−Eu(1)−Cl(1)	88.17(12)	N(3)−Eu(1)−N(6)	65.47(14)
O(2W)−Eu(1)−O(1W)	70.69(12)	O(1W)−Eu(1)−N(3)	75.67(15)	N(3)−Eu(1)−N(5)	128.95(16)	N(5)−Eu(1)−Cl(1)	81.87(12)	N(5)−Eu(1)−N(6)	63.51(14)
O(1)−Eu(1)−N(1)	107.57(14)	N(1)−Eu(1)−N(3)	90.26(16)	O(1)−Eu(1)−Cl(1)	90.47(10)	O(1)−Eu(1)−N(6)	139.34(12)	Cl(1)−Eu(1)−N(6)	76.34(9)
O(2W)−Eu(1)−N(1)	73.46(14)	O(1)−Eu(1)−N(5)	76.74(15)	O(2W)−Eu(1)−Cl(1)	147.31(10)	O(2W)−Eu(1)−N(6)	130.40(14)		
O(1W)−Eu(1)−N(1)	141.69(14)	O(2W)−Eu(1)−N(5)	124.39(14)	O(1W)−Eu(1)−Cl(1)	76.93(9)	O(1W)−Eu(1)−N(6)	132.93(11)		
				$Eu^{3+}C$					
Eu(1)−O(2)	2.552(5)	Eu(1)−O(1)	2.562(5)	Eu(1)−O(8)	2.570(5)	Eu(1)−N(1)	2.618(6)	Eu(1)−N(3)	2.682(6)
Eu(1)−O(5)	2.557(5)	Eu(1)−O(7)	2.564(4)	Eu(1)−O(4)	2.581(5)	Eu(1)−N(4)	2.680(6)	Eu(1)−N(5)	2.718(5)
O(2)−Eu(1)−O(5)	114.85(18)	O(1)−Eu(1)−N(4)	115.32(18)	O(5)−Eu(1)−O(7)	67.23(16)	O(7)−Eu(1)−O(4)	113.66(16)	O(2)−Eu(1)−N(5)	100.60(18)
O(2)−Eu(1)−O(1)	49.38(17)	O(7)−Eu(1)−N(4)	76.11(17)	O(1)−Eu(1)−O(7)	74.07(16)	O(8)−Eu(1)−O(4)	111.57(17)	O(5)−Eu(1)−N(5)	143.07(17)
O(5)−Eu(1)−O(1)	70.62(18)	O(8)−Eu(1)−N(4)	73.48(18)	O(2)−Eu(1)−O(8)	116.90(17)	O(2)−Eu(1)−N(1)	163.97(18)	O(1)−Eu(1)−N(5)	134.33(18)
O(2)−Eu(1)−O(7)	73.53(17)	O(4)−Eu(1)−N(4)	170.17(17)	O(5)−Eu(1)−O(8)	70.28(17)	O(5)−Eu(1)−N(1)	81.09(17)	O(7)−Eu(1)−N(5)	137.08(15)
O(7)−Eu(1)−N(1)	116.67(17)	N(1)−Eu(1)−N(4)	101.72(17)	O(1)−Eu(1)−O(8)	120.24(15)	O(1)−Eu(1)−N(1)	142.96(17)	O(8)−Eu(1)−N(5)	103.44(16)
O(8)−Eu(1)−N(1)	68.63(16)	O(2)−Eu(1)−N(3)	74.56(19)	O(7)−Eu(1)−O(8)	49.74(15)	O(8)−Eu(1)−N(3)	163.82(17)	O(4)−Eu(1)−N(5)	107.28(16)
O(4)−Eu(1)−N(1)	73.37(16)	O(5)−Eu(1)−N(3)	116.78(19)	O(2)−Eu(1)−O(4)	115.18(17)	O(4)−Eu(1)−N(3)	69.85(18)	N(1)−Eu(1)−N(5)	63.43(18)
O(2)−Eu(1)−N(4)	67.60(18)	O(1)−Eu(1)−N(3)	75.75(18)	O(5)−Eu(1)−O(4)	48.97(17)	N(1)−Eu(1)−N(3)	97.31(19)	N(4)−Eu(1)−N(5)	62.96(17)
O(5)−Eu(1)−N(4)	139.67(19)	O(7)−Eu(1)−N(3)	145.68(18)	O(1)−Eu(1)−O(4)	70.08(17)	N(4)−Eu(1)−N(3)	102.88(19)	N(3)−Eu(1)−N(5)	61.81(18)
				$Gd^{3+}C$					
Gd(1)−O(7)	2.551(5)	Gd(1)−O(1)	2.559(5)	Gd(1)−O(8)	2.565(5)	Gd(1)−N(1)	2.622(6)	Gd(1)−N(5)	2.717(6)
Gd(1)−O(2)	2.556(6)	Gd(1)−O(5)	2.559(5)	Gd(1)−O(4)	2.572(5)	Gd(1)−N(3)	2.682(6)	Gd(1)−N(5)	2.717(6)
				$Tb^{3+}C$					
Tb(1)−O(4)	2.465(7)	Tb(1)−O(5)	2.488(9)	Tb(1)−O(8)	2.500(8)	Tb(1)−N(1)	2.581(10)	Tb(1)−N(3)	2.638(10)
Tb(1)−O(1)	2.471(7)	Tb(1)−O(2)	2.488(8)	Tb(1)−O(7)	2.507(9)	Tb(1)−N(4)	2.648(9)	Tb(1)−N(5)	2.662(8)

central metal ions in the **A** complexes are also due to the bulkiness of the antipyrine molecules. As shown in the structures of the LnL^1 (Ln = Sm, Gd) complexes,[22] there is no water molecule coordinated to the metal ion.

For all complexes, the ligands L^1 and L^2 exhibit a tripodal coordination mode, with three imino nitrogen atoms (from pyridyl and benzimidazolyl groups) and one amino nitrogen atom as donors. Selected bond lengths and angles are given in Table 3. Like the LnL^1 complexes,[22] in the **A** and **B** complexes, the average $Ln-N_{imine}$ distances (i.e., 2.564 Å for $\mathbf{Pr^{3+}A}$ and 2.469 Å for $\mathbf{Eu^{3+}B}$) are significantly shorter than $Ln-N_{amine}$ distances (i.e., 2.770 Å for $\mathbf{Pr^{3+}A}$ and 2.728 Å for $\mathbf{Eu^{3+}B}$). But in the **C** complexes, the difference between the average $Ln-N_{imine}$ (i.e., 2.660 Å for $\mathbf{Eu^{3+}C}$) and $Ln-N_{amine}$ (i.e., 2.718 Å for $\mathbf{Eu^{3+}C}$) distances is not as much as in the **A** and **B** complexes, showing the subtle difference of coordination formed between L^1 and L^2. The structures of the **C** complexes are similar to those of their analogous 10-coordinate complexes LnL^1, but taking into account the difference in ionic radii, the average Ln−N distances of the **C** complexes (i.e., 2.675 Å for $\mathbf{Eu^{3+}C}$) are longer than those of LnL^1 (i.e., 2.623 Å for Sm), indicating that replacement of one benzimidazole by pyridine decreases the cavity size of the tripodal ligand L^2 and prevents a closer approach of the Ln^{3+}. A similar phenomenon was reported for the substituted bis(benzimidazolyl)pyridine ligands.[30]

Table 4. ^{1}H NMR Data for the Ligand L^2 and Complexes $\mathbf{La}^{3+}\mathbf{A}$ and $\mathbf{La}^{3+}\mathbf{C}$ in CD_3CN[a]

	δ_{H10}	δ_{H1}	$\delta_{H3,4}$	δ_{H8}	δ_{H6}	$\delta_{H2,5}$	δ_{H7}	δ_{H9}
L^1	3.91 (s)	4.03 (s)	7.20 (m)	7.25 (t)	7.48 (d)	7.59 (m)	7.69 (t)	8.61 (d)
L^2	4.24 (s)	4.52 (s)	7.23 (m)	7.27 (dd)	7.46 (d)	7.58 (m)	7.75 (t)	8.56 (d)
$\mathbf{La}^{3+}\mathbf{A}$	3.72 (s)	3.90 (d), 3.94(d)	7.18 (m)	6.57 (dd)	7.07 (d)	7.45 (m)	7.44 (m)	7.70 (m)
$\mathbf{La}^{3+}\mathbf{C}$	4.16 (d), 4.26(d)	4.18 (s)	7.29 (m)	7.44 (m)	7.46 (d)	(7.51 (m), 7.90 (m))	7.92 (m)	8.70 (d)

[a] Abbreviations: m, multiplet; s, singlet; d, double; t, triplet.

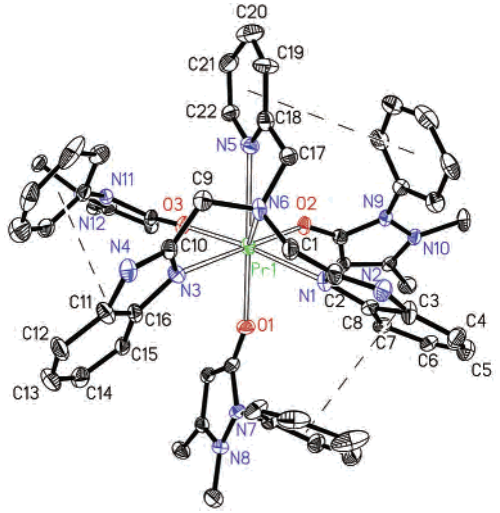

Figure 3. Crystal structure of $\mathbf{Pr}^{3+}\mathbf{A}$. ($\mathbf{Y}^{3+}\mathbf{A}$ is isostructural and isomorphous.)

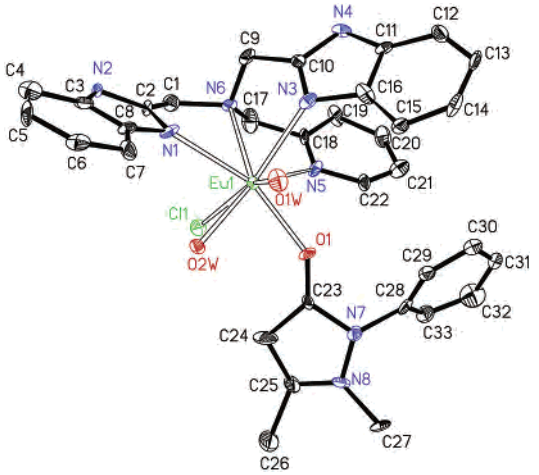

Figure 4. Crystal structure of $\mathbf{Eu}^{3+}\mathbf{B}$.

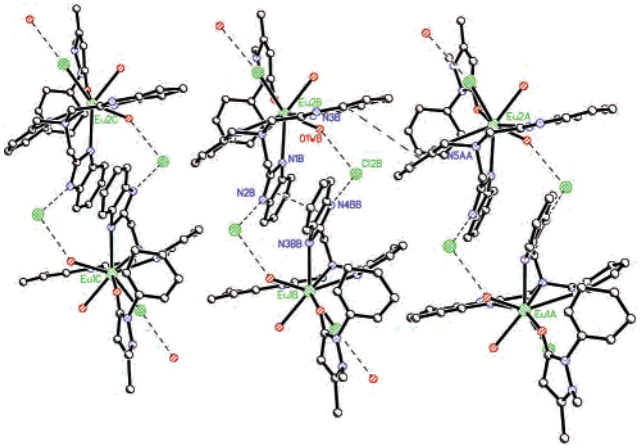

Figure 5. 2D layer generated by the intermolecular $\pi\angle\pi$ interactions and hydrogen bonds Cl···H−N (O) in $\mathbf{Eu}^{3+}\mathbf{B}$.

Meanwhile, it is noteworthy that, for all complexes, the Ln−N(bzim) distances are shorter than the Ln−N(py) distances, especially for the complexes of L^1 by ca. 0.1 Å on average, indicating that the benzimidazolyl group is favorable to be close to the metal ion and shows a stronger σ-donor than the pyridyl group, which is in agreement with the known pK_a values of 2-benzimidazolylmethyl (6.2) and pyridine (5.2).[31] This has important consequences for the luminescence characteristics of these complexes (see later).

The average Ln−O (nitrate) distances in the **C** complexes are within standard values (i.e., 2.564 Å for $\mathbf{Eu}^{3+}\mathbf{C}$), comparable to those in the tripodal analogue LnL^1 (i.e., 2.534 Å for Sm) and $[Ln(ntb)(NO_3)_3]\cdot H_2O$ (Ce−O 2.597 Å, Er−O 2.473 Å),[19,22] taking into account the difference in ionic radii.

As previously reported, the tripodal ligand L^1 also exhibits two kinds of configurations in these complexes. In the **A** complexes, with the three heterocyclic rings deflecting to the same direction and apart from each other at similar distances (Figure 3), the ligand L^1 shows a fanlike configuration.[22] The distances between the centroids of the three rings (i.e., 6.832, 6.910, and 7.547 Å for $\mathbf{Pr}^{3+}\mathbf{A}$) and the angles N_{imine}−Ln−N_{imine} (i.e., 96.8°, 100.3°, and 105.2° for $\mathbf{Pr}^{3+}\mathbf{A}$) are similar. Three antipyrine molecules are also apart from each other at similar distances. Every benzyl ring inclines parallel to one of the three heterocyclic rings of L^1 (average center-to-center distance 3.789 Å and average dihedral angle 4.8° for $\mathbf{Pr}^{3+}\mathbf{A}$), resulting in intramolecule $\pi-\pi$ stacking interactions that consequently affect the ^{1}H NMR of $\mathbf{La}^{3+}\mathbf{A}$ (see later). However, in $\mathbf{Eu}^{3+}\mathbf{B}$, with the pyridyl ring deflecting to the opposite direction to the two benzimidazolyl rings and inclining to the benzimidazolyl ring containing N(3), the ligand L^1 shows a pincer-like configuration,[22] so the centroid-to-centroid distances of the three rings (3.961, 7.283, and 7.945 Å) and the N_{imine}–Ln−N_{imine} angles (67.7°, 90.3°, and 128.9°) are quite different from each other (Figure 4). Similar to complexes $[LnL^1Cl_3(H_2O)]$,[22] weak intramolecular $\pi\angle\pi$ stacking interaction exists in $\mathbf{Eu}^{3+}\mathbf{B}$, with a center-to-center distance between the pyridlyl ring and the adjacent benzimidazolyl ring of 3.96 Å and a dihedral angle of 29.8°. In the meantime, as shown in Figure 5, two kinds of weak intermolecular $\pi-\pi$ stacking interactions of benzimidazole(N_{1B})−benzimidazole(N_{4BB}) and benzimidazole(N_{3B})−pyridine(N_{5AA}) are found between two neighboring molecules, with center-to-center distances of 3.74 and 3.89 Å (dihedral angles 9.7° and 13.4°), respec-

(30) Petoud, S.; Bünzli, J.-C. G.; Schenk, K. J.; Piguet, C. *Inorg. Chem.* **1997**, *36*, 1345.
(31) Robert, C. W. *Handbook of Chemistry and Physics*; The Chemical Rubber Co.: 1969; Vol. 50, p 115.

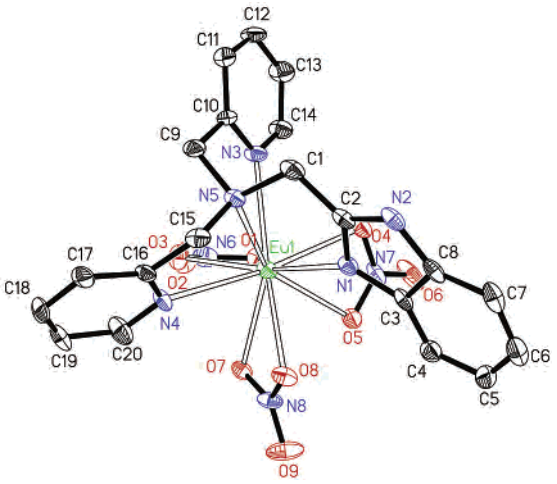

Figure 6. Crystal structure of $\mathbf{Eu}^{3+}\mathbf{C}$. (The $\mathbf{Gd}^{3+}\mathbf{C}$ and $\mathbf{Tb}^{3+}\mathbf{C}$ complexes are isostructural and isomorphous.)

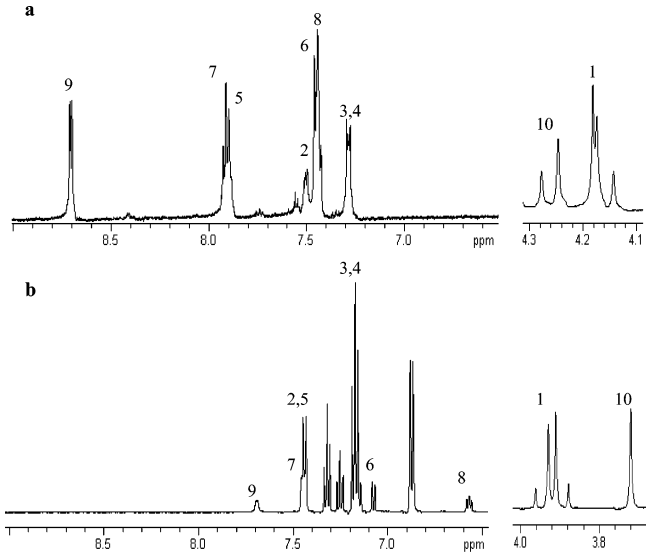

Figure 7. ^{1}H NMR spectra of the the $\mathbf{La}^{3+}\mathbf{C}$ (a) and $\mathbf{Gd}^{3+}\mathbf{A}$ (b) complexes in CD_3CN at 298 K.

tively, together with two kinds of hydrogen bondings of Cl···H−N (Cl_{2B}···N_{4BB} 3.141 Å) and Cl···H−O (Cl_{2B}···O_{1WB} 3.039 Å), forming a two-dimensional layer. Comparison of the structures of these complexes of L^1 shows that adaptation of the more steric pincer-like configuration favors intra- and intermolecular $\pi-\pi$ stacking interaction, which in return stabilizes this kind of configuration.[22] In the **C** complexes, the tripodal ligand L^2 exhibits the same fanlike configuration as in the **A** complexes, with similar distances between the centroids of the three rings (i.e., 6.188, 6.705, and 6.897 Å for $\mathbf{Eu}^{3+}\mathbf{C}$) and N_{imine}–Ln−N_{imine} angles (i.e., 97.3°, 101.7°, and 102.9° for $\mathbf{Eu}^{3+}\mathbf{C}$) (Figure 6).

The IR spectra show that, for all complexes, the low-energy absorption band of C═N stretching for the tripodal ligand blue shifts to about 1606 cm^{-1} as compared to its counterpart for the free ligand, showing the coordination of the tripodal ligand.[32] For the **A** and **B** complexes, the intense absorption bands of C═O appear in the range 1625−1632 cm^{-1}, which red shift compared to those of free antipyrine (1665 cm^{-1}),[33] showing the coordination of antipyrine. For the **A** complexes, the ClO_4^- anions show the two vibrations typical of ionic perchlorate (1095 and 625 cm^{-1}), and for the **C** complexes, two intense absorptions associated with the asymmetric stretching of NO_3^- appear in the ranges 1294−1301 (ν_4) and 1460−1475 (ν_1) cm^{-1}, clearly establishing that the NO_3^- groups (C_{2v}) are bidentate coordinated.[34]

^{1}H NMR and Conductivity Studies in Solution. The ^{1}H NMR spectra of the free ligand L^2 and the diamagnetic lanthanum(III) complexes $\mathbf{La}^{3+}\mathbf{A}$ and $\mathbf{La}^{3+}\mathbf{C}$ were measured in CD_3CN. The chemical shift data are given in Table 4. The chemical shift data of the free ligand L^1 have been reported before and are shown here for comparison with those of $\mathbf{La}^{3+}\mathbf{A}$. The ^{1}H NMR spectra of the complexes are shown in Figure 7. Upon coordination with metal ion, the heterocyclic proton resonances of L^2 in $\mathbf{La}^{3+}\mathbf{C}$ shift to lower field as compared to those of free L^2. However, the heterocyclic proton resonances of L^1 in $\mathbf{La}^{3+}\mathbf{A}$ oppositely shift to higher field as compared to those of free L^1. This can be explained by the difference between their structures. As shown in the crystal structures of the **A** complexes (Figure 3), since three benzol rings of antipyrine molecules incline parallel to the heterocyclic rings of L^1, all heterocyclic hydrogens of L^1 lie in the antimagnetic section of the benzol rings, so their resonances shift to higher field. This kind of higher field shift has been discussed by Aoki's group.[35]

It is interesting that, in complex $\mathbf{La}^{3+}\mathbf{A}$ (or $\mathbf{La}^{3+}\mathbf{C}$), two H^{10} (or H^1) protons of L^1 (or L^2) exhibit a singlet as free ligand; however, another two H^1 (or H^{10}) protons of L^1 (or L^2) show an "AB" quartet, with an intensity rato of A_1 to B_1 of 0.26 (or 0.56), which is comparable to the calculated data, 0.24 (or 0.53). In solution, rapid inversion of the central amino nitrogen atom of the free ligand L^1 (or L^2) leads to an average C_{2v} symmetry. In this case, we expect only enantiotopic methylene protons. Thus, the H^{10} (or H^1) protons show only one singlet. Upon coordination, the inversion of the capping nitrogen atom is blocked by complexation and the average C_s symmetry is restored, thus leading to the expected singlet for the H^{10} (or H^1) protons and AB quartet for the H^1 (or H^{10}) protons of the ligand L^1 (or L^2). As shown in crystal structures of the **A** (or **C**) complexes (Figures 3 and 6), there is an approximate (noncrystallographic) plane of symmetry passing through the arm including H^{10} (or H^1) of the ligand L^1 (or L^2),[36] so two H^{10} (or H^1) protons have the same chemical environments and show a singlet. In contrast the chemical environments between two H^1 (or H^{10}) protons is somewhat different and shows an "AB" quartet. The ^{1}H NMR of the **A** and **C** complexes show that the tripodal ligands have similar configuration in the solution and solid states. It is well-known that, for this kind of half-

(32) Thompson, L. K.; Ramaswamy, B. S.; Seymour, E. A. *Can. J. Chem.* **1997**, *55*, 880.
(33) *Standard Infrared Grating Spectra*; Vols. 9 and 10, p 8399.
(34) Carnall, W. T.; Siegel, S.; Ferrano, J. K.; Tani, B.; Gebert, E. *Inorg. Chem.* **1973**, *12*, 560.
(35) Murayama, K.; Aoki, K. *Chem. Commun.* **1998**, 607.
(36) Reeves, Z. R.; V. Mann, K. L.; Jeffery, J. C.; Cleverty, J. A. M.; Ward, M. D.; Barigelletti, F.; Armaroii, N. *J. Chem. Soc., Dalton Trans.* **1999**, 349.

hard tripodal ligand, keeping a rigid conformation with the central ion is favorable to designing a luminescent lanthanide complex.[7]

Seeking to know more about the complexes in different solvents, we measured the conductivities of the **B** and **C** complexes in CH_3OH and CH_3CN (Table 1). In CH_3OH, the molar conductivities for the **B** and **C** complexes lie in the ranges 300−360 and 180−230 $S\cdot cm^2\cdot mol^{-1}$, respectively, indicating that the **B** and **C** complexes are 3:1 and 2:1 electrolytes.[37] Meanwhile, we measured the conductivities of complexes $\mathbf{Dy}^{3+}\mathbf{B}$ and $\mathbf{Sm}^{3+}\mathbf{C}$ in the range 1×10^{-3} to 1×10^{-6} M. For strong electrolytes, $\Lambda_e = \Lambda_o - BC_{eq}^{1/2}$,[38−40] in which Λ_e is the equivalent conductivity, Λ_o is the equivalent conductivity at infinite dilution, and C_{eq} is the equivalent concentration. For the complex $\mathbf{Dy}^{3+}\mathbf{B}$, a plot of $\Lambda_o - \Lambda_e$ vs $C_{eq}^{1/2}$ gave an experimental slope of 953 ± 92 $S\cdot L^{1/2}\cdot equiv^{-1/2}$. This value compared favorably to the theoretical slope 889 $S\cdot L^{1/2}\cdot equiv^{-1/2}$ determined from the Kohlraush and Onsager equations for a 3:1 electrolyte.[39] Similarly, complex $\mathbf{Sm}^{3+}\mathbf{C}$ gave an experimental slope of 692 ± 76 $S\cdot L^{1/2}\cdot equiv^{-1/2}$, which compared favorably with the theoretical slope 618 $S\cdot L^{1/2}\cdot equiv^{-1/2}$ for a 2:1 electrolyte. The above data suggest that for the **B** complexes, the coordinated Cl^- dissociates from the metal ion. And for the **C** complexes, two nitrates are replaced by *q* methanol molecules, forming $[LnL^1(NO_3)(CH_3OH)_q](NO_3)_2$. For steric reasons, it is unlikely that the two nitrates would be replaced by four methanol molecules for the **C** complexes, and the value of *q* is determined from its luminescence studies (see later).

In CH_3CN, the molar conductivities of the **B** complexes lie in the region 170−210 Ω^{-1} cm^2 mol^{-1}, indicating that all complexes are 2:1 electrolytes with the coordination of Cl^- remaining constant. For the **C** complexes, the molar conductivities in CH_3CN are about 100 times smaller than in methanol, indicating the complexes remain intact and therefore neutral.

The results of ^1H NMR and conductivity measurements show that, in the moderately polar CH_3CN, the complexes remain intact and, in CH_3OH, the anions dissociate, although the tripodal ligand still coordinates. It is seen that there is likely competition between the solvent and the ligand for the lanthanide ion, and a similar phenomenon was found in the complexes of heptadentate N_4O_3 Schiff base and some similar tripodal ligands.[13,18,22]

Luminescence Properties of the Complexes. The photophysical properties of free ligand L^1 and its nitrate-coordinated complexes LnL^1 (Ln = Eu, Tb) at 298 K have been reported before and are included here in the discussion for comparison purposes (Figure 8). The photophysical properties of $Gd^{3+}L^1$ are reported here for the first time.

All complexes can be dissolved in CH_3CN and are thermally stable in solvent, as shown by the lack of changes

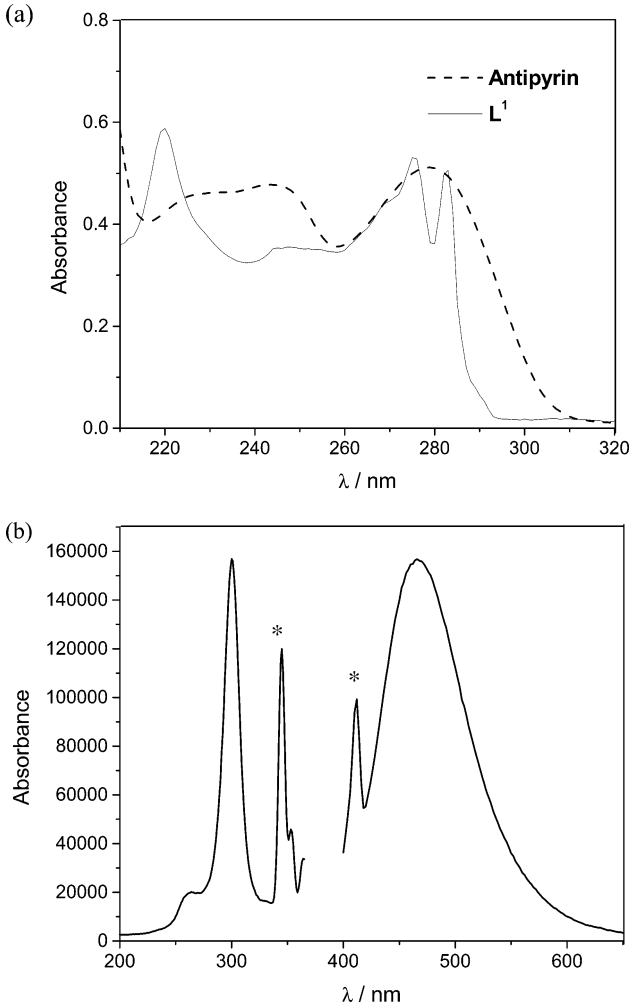

Figure 8. (a) Absorption spectra of the ligand L^1 (—) and antipyrine (---) in CD_3CN. (b) Excitation (monitored at 465 nm) and emission spectra of antipyrine in CH_3CN at 298 K. The peaks marked with an asterisk are due to scattering.

in the absorption and luminescence spectra. The absorption spectra of free L^2, $\mathbf{Tb}^{3+}\mathbf{C}$, and $\mathbf{Eu}^{3+}\mathbf{A}$ in CH_3CN are shown in Figure 9a. Free L^2 exhibits absorption bands at 213, 251, 276, and 281 nm, which are strongly perturbed upon coordination to Ln^{3+} in the **C** complexes, implying coordination of the ligand.[41] All **A**, **B**, and **C** complexes display almost identical spectral profiles, and the **A** and **B** complexes also display the absorption bands of antipyrine, which overlap with those of L^1.

Free tripodal ligands L^1 and L^2 exhibit an intense, short-lived UV fluorescence in CH_3CN solution, which, in a rigid matrix at 77 K, is accompanied by a strong, long-lived, and structured phosphorescence band (Table 5). These emissions are due to the deactivation of the lowest electronic singlet and triplet states. GdL^1 and $\mathbf{Gd}^{3+}\mathbf{C}$ complexes display a ligand-centered (LC) fluorescence both at room temperature and at 77 K, and LC phosphorescence at 77 K only (Table 5, Figure 10). This is an expected result since the metal-centered (MC) electronic levels of Gd^{3+} (>31000 cm^{-1}) are typically well above the ligand-centered electronic levels of

(37) Geary, W. J. *Coord. Chem. Rev.* **1971**, *7*, 81.
(38) Feltham, R. D.; Hayter, R. G. *J. Chem. Soc.* **1964**, 4587.
(39) Boggess, R. K.; Zatko, D. A. *J. Chem. Educ*. **1975**, *52*, 649.
(40) Rillema, D. P.; Callahan, R. W.; Mack K. B. *Inorg. Chem*. **1982**, *21*, 2589.
(41) Piguet, C.; Williams, A. F.; Bernardinelli, G.; Moret, E.; Bünzli, J.-C. G. *Helv. Chim. Acta* **1992**, *75*, 1697.

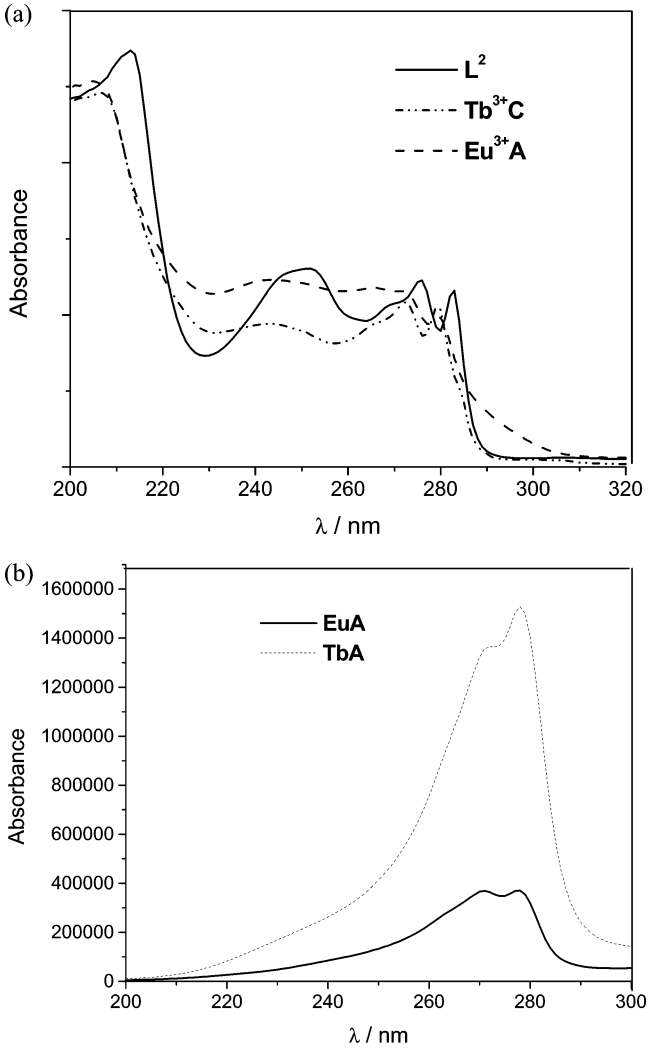

Figure 9. (a) Absorption spectra of the ligand L^2 (—), **Tb**$^{3+}$**C** (— ·· —), and **Eu**$^{3+}$**A** (---) in CH_3CN. (b) Excitation spectra of **Eu**$^{3+}$**A** (—, monitored at 613 nm) and **Tb**$^{3+}$**A** (---, monitored at 543 nm) in CH_3CN at 298 K.

Table 5. Luminescence Properties of the Ligands and Their Gd(III) Complexes in CH_3CN in 298 and 77 K

	^{1}LC^a (298 K)			^{3}LC^a (77 K)	
	λ_{max}	τ (ns)	Φ_{em}	λ_{max}	τ (ms)
L^1	*376*^{b}	3.9	0.250	478	960
GdL^1	382	1.1	0.013	489	8.4
L^2	351	2.7	0.170	453	850
GdL^2	367	0.8	0.015	462	5.1

^{a} ^{1}LC and ^{3}LC are the lowest spin-allowed and the lowest spin-forbidden ligand-centered ($\pi \rightarrow \pi^*$) excited states, respectively. ^{b} Data taken from ref 22 and included for comparison purposes.

aromatic ligands.[42] Therefore, ligand-to-metal energy transfer and the consequent MC luminescence cannot be observed. The lower fluorescence quantum yield and the shorter phosphorescence lifetime exhibited by the GdL^1 and **Gd**$^{3+}$**C** complexes compared to free L^1 and L^2, respectively, indicate that the heavy ion facilitates intersystem crossing processes. In the meantime, from the highest energy vibrational feature of the phosphorescence bands of the $Gd^{3+}L^1$ and **Gd**$^{3+}$**C** complexes, the zero−zero energy of the lowest ligand-centered excited triplet state (^{3}LC) is estimated to be about 23600 and 23800 cm^{-1}, respectively, and these values can be taken also for the Eu^{3+} and Tb^{3+} analogues.[43,44] In the **Gd**$^{3+}$**A** and **Gd**$^{3+}$**B** complexes, since the emission peaks of L^1 overlap with those of antipyrine, the ^{3}LC state cannot be determined as for the above two complexes. But in view of the similar coordination of L^1 in these complexes, it can be estimated by that of $Gd^{3+}L^1$ (see later).

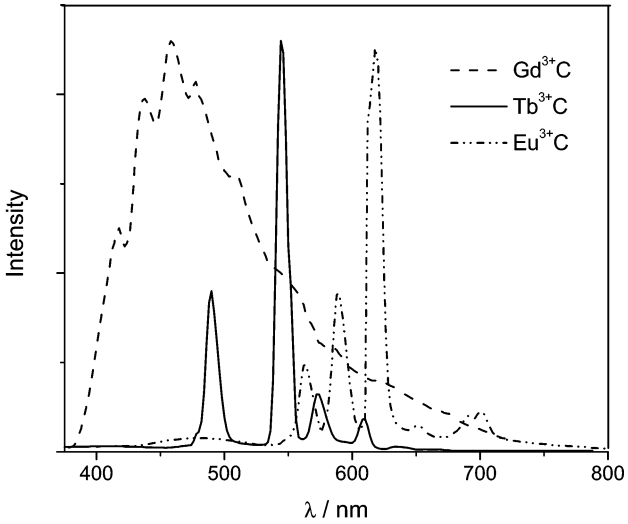

Figure 10. Emission spectra of **Gd**$^{3+}$**C** (---) in a CH_3CN rigid matrix at 77 K and **Tb**$^{3+}$**C** (—) and **Eu**$^{3+}$**C** (— ·· —) in CH_3CN at 298 K.

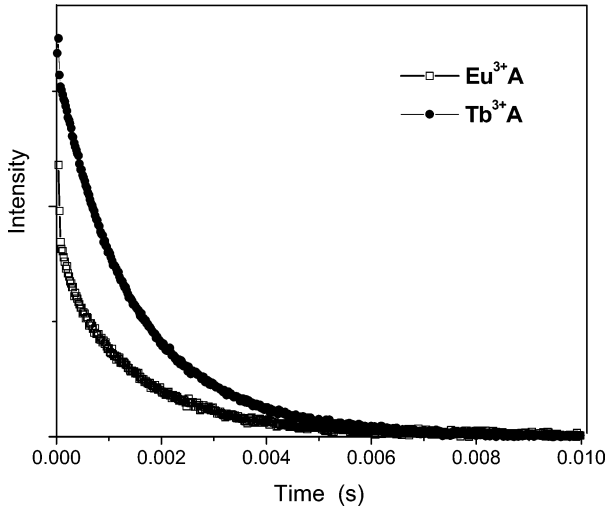

Figure 11. Decay curves of complexes **Eu**$^{3+}$**A** (□) and **Tb**$^{3+}$**A** (●) in CH_3CN.

For all Tb^{3+} and Eu^{3+} complexes, the typical narrow emission bands of the Eu^{3+} and Tb^{3+} ions can be detected upon excitation of the ligand-centered absorption band, and the ligand-centered luminescence is completely suppressed, showing that ligand-to-metal energy transfer takes place efficiently (Figure 10). The absorption and excitation (monitored at 613 nm) spectra of **Eu**$^{3+}$**A** are shown in parts a and b, respectively, of Figure 9. The absorption bands coincide with the excitation bands, revealing the origin of the physical

(42) Reisfeld, R.; Jorgensen, C. K. *Lasers and Excited States of Rare Earths*; Springer: Berlin, 1977.

(43) Martin, N.; Bünzli, J.-C. G.; McKee, V.; Piguet, C.; Bernardinelli, C.; Hopfgartner, G. *Inorg. Chem.* **1998**, *37*, 577.

(44) Elhabiri, M.; Scopelliti, R.; Bünzli; J.-C. G.; Piguet; C. *J. Am. Chem. Soc*. **1999**, *121*, 10747.

Table 6. Quantum Yields (Φ_{Em}), Luminescence Lifetime (τ), and Derived Solvation Values (q) for the Eu(III) and Tb(III) Complexes

		τ^a (ms)				
	$\Phi_{em}{}^b$	CH_3CN^d	CH_3CN^e	CH_3OH^e	CD_3OD^e	$q(CH_3OH)$
$EuL^{1\,c}$	0.031	0.73	0.36	0.81	3.2	
$TbL^{1\,c}$	0.380	1.14	0.95	1.57	3.5	
Eu^{3+}**A**	0.097	1.56	0.91	0.82	0.93	<0.5
Tb^{3+}**A**	0.420	1.69	1.62	1.56	1.66	<0.5
Eu^{3+}**B**	0.016	0.95	0.50	0.33	0.64	3.1
Tb^{3+}**B**	0.210	1.27	1.23	0.65	0.87	3.3
Eu^{3+}**C**	0.190	1.02	0.67	0.30	0.58	3.4
Tb^{3+}**C**	0.273	1.25	1.30	0.78	1.15	3.5

[a] Measured in correspondence with the most intense emission band ($^5D_4 \rightarrow {}^7F_5$ for Tb^{3+} and $^5D_0 \rightarrow {}^7F_2$ Eu^{3+}). [b] Measured in CH_3CN at 298 K. [c] Data taken from ref 22. [d] Measured at 77 K. [e] Measured at 298 K.

process measured. Meanwhile, the complete quench of the luminescence of antipyrine (at 465 nm, Figure 8b) for the **A** and **B** complexes shows that in solution antipyrine molecules remain coordinated and efficiently transfer energy to lanthanide ions.[45] The emission quantum yield and lifetime data in different solvents are reported in Table 6. The linear fit analysis of the experimental data shows the decay is monoexponential for all Eu^{3+} and Tb^{3+} complexes (Figure 10). It shows that in contrast to the **A** complexes, the **B** and **C** complexes show considerably shorter lifetimes of the metal-centered emissions in methanol than in CH_3CN. As studied by ^1H NMR and conductivity measurements, the **B** and **C** complexes are stable in CH_3CN, so that solvent-based quenching is restricted to outer-sphere effects. However, in CH_3OH, one chloride dissociates for the **B** complexes and two nitrates dissociate for the **C** complexes. At the same time, methanol molecules, which can efficiently quench lanthanide luminescence, enter the coordination sphere. The number of coordinated methanol molecules (q) as determined by the Horrocks equation is given in Table 6.[7] With the results of the conductivity study (see above) and the error in q (± 0.5), the average values of 3.4 for the **B** complexes and 3.5 for the **C** complexes suggest three methanol molecules enter the coordination sphere and form $[LnL^1(antipy)(CH_3OH)_3]Cl_3$ and $[LnL^2(NO_3)(CH_3OH)_3][NO_3]_2$, respectively. In the former two waters are replaced by two methanol molecules. A similar phenomenon was reported for LnL^1 complexes in which $[LnL^1(NO_3)(CH_3OH)_3][NO_3]_2$ was formed in methanol.[22] For the **A** complexes, the small change in lifetimes in CH_3OH and CD_3OD indicates that the complexes are stable and no solvent molecule enters the coordination sphere. The ability for antipyrine to stabilize the structures of the complexes and keep the solvent molecules out of the ion coordination sphere is favorable to increasing the luminescence of the complexes.[7,46]

Although with the same ligand L^2 and antipyrine, the **A** complexes have considerably longer lifetimes and higher quantum yields than the **B** complexes. this is evident from the fact that the coordinated water molecule in the latter partially quench the luminescence and decrease the values of τ and Φ. Through vibronic coupling with the vibrational states of the O−H oscillators, efficient nonradiative deactivations take place in the lanthanide active state.[46] Using the emission lifetimes of the **B** complexes in CH_3CN before and after addition of a few drops of D_2O that will exchange with the water molecule, the number of coordinated water molecules is determined.[47] The values of 0.9 for $\mathbf{Eu}^{3+}\mathbf{B}$ and 0.8 for $\mathbf{Tb}^{3+}\mathbf{B}$ suggest one water molecule is coordinated in CH_3CN, in good agreement with the crystallographic analyses. Meanwhile, $\mathbf{Tb}^{3+}\mathbf{A}$ and $\mathbf{Eu}^{3+}\mathbf{A}$ have the longest lifetime and highest quantum yield in the respective series of Tb^{3+} and Eu^{3+} complexes. As shown in the crystal structures and emission spectra of the **A** complexes, three big antipyrine molecules not only prevent water molecules from entering the coordination sphere but also efficiently transfer energy to metal and thus increase the lanthanide luminescence.

In every series of complexes, the Tb^{3+} complexes have a longer lifetime and higher quantum than the Eu^{3+} complexes, regardless of the solvent. As shown by Reinhoudt and Latva et al.,[48−50] for the Eu^{3+} and Tb^{3+} complexes, the ^{3}LC state must be 3500 cm^{-1} above the Ln^{3+} excited state to ensure efficient energy transfer. On the other hand, efficient back-transfer takes place in the Tb^{3+} complexes when $\Delta E(^3LC-{}^5D_4) < 1850$ cm^{-1}. For the $Tb^{3+}L^1$ and $\mathbf{Tb}^{3+}\mathbf{C}$ complexes, the energy gap between the luminescent $^5D_0$ level (20400 cm^{-1}) and the ^{3}LC level (23600 cm^{-1} for $Tb^{3+}L^1$ and 23800 $cm^{-1}$for $\mathbf{Tb}^{3+}\mathbf{C}$; see above) is larger than 3200 cm^{-1}, so the back-energy-transfer process to the ^{3}LC state is negligible and these complexes show better emission. Although the ^{3}LC level of $\mathbf{Tb}^{3+}\mathbf{A}$ and $\mathbf{Tb}^{3+}\mathbf{B}$ cannot be directly confirmed, considering the similar coordination of L^1 in $Gd^{3+}L^1$, it is established that the thermally activated back-energy-transfer process can also be negligible in these two complexes. Meanwhile, this is confirmed by the fact that the luminescence lifetimes for the Tb^{3+} complexes are similar at 77 and 298 K in CH_3CN. This kind of back-energy-transfer process in Tb^{3+} complexes is not so significant in Eu^{3+} complexes, because the energy gap between the MC level $^5D_1$ (19000 cm^{-1}) and the ^{3}LC level is well above 4600 cm^{-1} in every case. In Table 6, the lifetime of the Eu^{3+} complexes at 77 K is much longer than that at 298 K in CH_3CN, indicating the thermal transfer of the ligand excitation energy to the low-lying ligand-to-metal charge-transfer (LMCT) excited state,[51] which decreases the lanthanide luminescence. As shown in crystallographic results, the benzimidazole nitrogen atom has better donating properties than the pyridine nitrogen atom and the ligand L^1 can approach closer to the central ion. So this undesired radiationless pathway will be favored for L^1 relative to L^2,[42,51] and for the similar 10-coordinated lanthanide complexes $\mathbf{Eu}^{3+}\mathbf{C}$ and $Eu^{3+}L^1$, the former has higher

(45) Piguet, C.; Hopfgartner, G.; Williams, A. F.; Bünzli, J.-C. G. *Chem. Commun*. **1995**, 491.
(46) Horrocks, W. D.; Sudnick, D. R. *Acc. Chem. Res.* **1981**, *14*, 384.
(47) Reeves, Z. R.; Mann, K. L. V.; Jeffery, J. C.; Cleverty, J. A. M.; Ward, M. D.; Barigelletti, F.; Armaroii, N. *J. Chem. Soc., Dalton Trans.* **1999**, 349.
(48) Steemers, F. J.; Verboom, W.; Reinhoudt, D. N.; Vandertol, E. B.; Verhoeven, J. W. *J. Am. Chem. Soc.* **1995**, *117*, 9408.
(49) Latva, M.; Takalo, H.; Mukkala, V. M.; Matachescu, C.; Rodriguez-Ubis, J.-C.; Kankare, J. *J. Luminesc.* **1997**, *75*, 149.
(50) Petoud, S.; Glanzmann, T.; Bünzli, J.-C. G.; Piguet, C.; Qin, X.; Thummel, R. P. *J. Luminesc*. **1999**, *82*, 69.
(51) Aime, S.; Botta, M.; Fasano, M.; Terreno, E. *Chem. Soc. Rev*. **1998**, *27*, 19.

luminescence quantum yield than the latter (Table 6). On the other hand, as the reduction potential of Tb^{3+} (−3.5 V) is much higher than that of Eu^{3+} (−0.35 V),[52] this kind of nonradiative deactivation pathway is not relevant for Tb^{3+} complexes.

Conclusions

Three series of lanthanide(III) complexes have been prepared using two similar tripodal ligands bearing benzimidazole and pyridine groups, and six complexes have been structurally characterized. The anions (Cl^- and ClO_4^-) have a substantial effect on the structures of the **A** and **B** complexes. In the former, the central metal ions are completely encapsulated by chromophoric ligands (one L^1 and three antipyrine molecules) and show good luminescence character. However, there are two water molecules coordinated to the central ion in the latter, resulting in the decrease of the emission quantum yield and lifetime values.

These complexes exhibit varied luminescence properties, which can be rationalized on the basis of structural, electronic, and solvent-induced effects. For all Eu^{3+} and Tb^{3+} complexes, the complete suppression of the ligand-centered luminescence enhances the ligand-to-metal energy transfer. Because of the solvent-based quenching, for the **B** and **C** complexes the lifetimes of metal-centered emission in methanol are considerably shorter than in CH_3CN. A conductivity study in methanol and comparison of the emission lifetimes of the Eu^{3+} and Tb^{3+} complexes in CH_3OH and CD_3OD suggest the formation of $[LnL^1(antipy)(CH_3OH)_3]Cl_3$ and $[LnL^2(NO_3)(CH_3OH)_3][NO_3]_2$, respectively. Since the high-lying electronic ^3LC levels are present in the Tb^{3+} complexes, the nonradiative back-energy-transfer process between metal- and ligand-centered electronic levels is ineffective, while the thermally activated energy transfer from the initially generated ^3LC excited state to an LMCT excited state in Eu^{3+} complexes limits the efficiency of ligand-to-metal energy transfer and thereby lowers the luminescence output of these complexes. These results clearly show a wide range of ways for tuning the luminescence properties of lanthanide complexes.

Acknowledgment. Financial support from the National Natural Science Foundation of China, the State Key Laboratory of Rare Earth Materials Chemistry and Applications of Peking University, the Hong Kong Baptist University (Grant FRG/00-01/II-40), and the Hong Kong Research Grants Council is greatly appreciated.

Supporting Information Available: X-ray crystallographic data in CIF format. This material is available free of charge via the Internet at http://pubs.acs.org.

IC025799P

(52) Bard, A. J. In *Standard Potentials in Aqueous Solution*; Bard, A. J., Parsons, R., Jordan, J., Eds.; Marcel Dekker: New York, 1985.